Tissue Biopsy Dissociation

BME 301

May 2nd, 2018

Client: Dr. Sameer Mathur
University of Wisconsin Hospital

Advisor: Dr. Krishanu Saha
University of Wisconsin-Madison Department of Biomedical Engineering

Team Members:
Raven Brenneke (BSAC)
Thomas Guerin (BPAG)
Chrissy Kujawa (Communicator)
Nathan Richman (BWIG)
Lauren Ross (Team Leader)

Abstract

Biological research seeking to understand the pathophysiology of a disease often requires the use of individual cells. Our client conducts asthma research that necessitates obtaining white blood cells from lung tissue. Specifically, eosinophils are studied to understand the inflammatory processes of an asthmatic reaction. Successfully dissociating eosinophils from lung tissue biopsies allows researchers to develop new treatments options for asthma patients, improving their outcomes. The current device being used for this process is the Miltenyi GentleMACS™ Dissociator, which has not yielded the number of viable cells necessary for analysis. A small tissue biopsy, 12 mm^3 or less, is desired to minimize patient pain and reduce recovery time. This design team was tasked with creating a dissociation device that can successfully dissociate small tissue samples to yield viable cells that can be analyzed using flow cytometry. The device must yield at least 10,000 cells from a single biopsy. To accomplish this task, a microfluidic device that utilizes shear stress was 3D printed. Testing has shown that this device dissociates cells from frozen murine tissue at about 17,000 cells/mm^3 while testing on the GentleMACS™ yields about 36,000 cells/mm^3. From these values we can conclude that our device is able to dissociate lung biopsies of approximately 13 mm^3, but not as successfully as the GentleMACS™. Future testing should look at using fresh tissue samples, human samples, and ultimately test the difference between healthy and asthmatic human samples using flow cytometry.

I. Introduction

Motivation

The University of Wisconsin-Madison has a nationally known research facility for Asthma, Allergy, and Pulmonary Research. Asthma has been studied at UW Madison for over 30 years, producing over 400 research studies. These studies have investigated the role of genetics in asthma, treatment of asthma in children, and how colds affect asthma. Dr Sameer Mathur, the client for this project, studies a specific white blood cell type called eosinophils in the context of understanding the inflammatory process during an asthmatic response. The client's asthma research has significantly contributed to the development of new asthma medications and guidelines for treatment [1].

Asthma research requires the close study of cellular processes to understand the physiology behind the disease. Cells provide structure and function for all living things and house the biological machinery that make the proteins, chemicals, and signals for everything that happens within the body. There are about 200 major types of cells and they all function in different ways. Biologists rely on different types of tools to examine these cells and gain a better understanding of how they function. Learning more about how cells work, and what happens when they do not work properly, is imperative in understanding the biological processes that keep humans healthy [2].

Asthma affects nearly 1 in 12 people in the U.S. alone, with the number of affected individuals is rising each year, according to the CDC [3]. A disease this widespread leads to huge economic costs with approximately 56 billion dollars a year in medical expenses, lost work days, and premature deaths caused by asthma [3]. If this project can help the client better understand the mechanisms behind the asthmatic response, then it may lead to better treatments and prevention methods for asthma. Understanding and elucidating the causes of this disease are important for our society to live longer, healthier, and more productive lives.

Dr. Mathur’s research group at UW-Madison currently uses tissue dissociation as a method of studying individual cells to gain a better understanding of an asthmatic response. Lung biopsy procedures must be performed to obtain the desired tissue samples. After a biopsy procedure, the patient may experience pain at the site of biopsy during recovery. A study like this relies on volunteers, so patient comfort and recovery is very important. It is therefore desired to take the smallest biopsy possible to increase patient comfort while maintaining accurate and reliable results. By taking the smallest possible biopsy, the patient’s pain, discomfort, and recovery time will be reduced [4]. In order to make this a viable option, these smaller samples must be able to be dissociated into individual cells while maintaining the integrity of the cell, Creating a device that can do just that is the goal of this design project.

Existing Devices and Current Methods

Tissue dissociation is commonly performed in two different ways. The first of which is chemical dissociation. There are several different protocols for chemical dissociation that vary with tissue type, but they usually follow the same set of steps. First, the tissue is placed in a specific concentration of collagenase and enzyme solution to break down the extracellular matrix of the tissue. Next, the solution is heated to an optimal temperature and incubated with gentle vortexing or mixing. Once this is complete, a filter is used to "strain" the solution and obtain certain types of cells. This is a very common method, but there are some drawbacks, mostly with inconsistency of cell yields and disruption of cell characteristics due to the enzymes used. What many researchers do instead is to use mechanical dissociation, or a combination of both chemical and mechanical dissociation. A handful of mechanical dissociation products are outlined below.

A well known mechanical tissue dissociation device is the gentleMACS™ Dissociator (Figure 1). This benchtop instrument is meant to perform a semi-automated dissociation of tissues into single-cell suspensions. It can process one to two samples at a time. There are two types of unique tubes that can be used with this instrument and each tube has a rotor that moves over teeth on the stator to perform mechanical grinding with rotation (Figure 2).

Figure 1. GentleMACS™ Dissociation Device. A dissociation tube is place in the opening at the top, an automatic cycle is then selected with the buttons and display at the bottom.

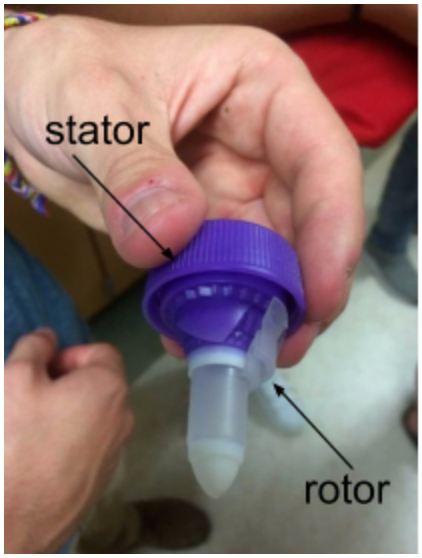

Figure 2. Conical Tube used with grinding teeth used in the gentleMACS™ system to dissociate tissue.

This device has several settings for different dissociation process cycles, and special protocols have been developed by the company for dissociation of specific tissues [5]. This

device was previously used in the lab to dissociate tissue samples, but due to the size of the tube and grinding teeth, the client said the device was unable to successfully dissociate the small biopsies he receives from patients. The protocol used for this device can be found Appendix B.

To solve the issues of other dissociation devices, researchers have started creating their own microfluidic dissociation devices. The idea behind these microfluidic devices is to push a small amount of solution and tissue through a small space which creates shear force on the tissue which should take off individual cells.

The first microfluidic device examined for this project was created to dissociate tumor cell aggregates. Its novel design utilized a series of channels that halved in size until the smallest channel was 125 μm in width. The walls of the channels have smooth constrictions that reduce liquid vortices that may trap cells (Figure 3). The device uses pressurized air to force tissue samples that are in solution through channels which causes gradients of velocity to form that produce shear forces strong enough to break apart cell aggregates. This device has been shown to work for tumor cells and cell aggregates [6]. This design still utilizes enzymes to help loosen cells, but once they are put in the device they are subject to maximum shear forces of 9 dyne/cm^2 (0.9 Pa) found in the smallest channels. They found that the best method was to run their cells through the device 10 times in order to obtain the most individual cells. To create this product they used laser cutting to create seven layers and glued them together.

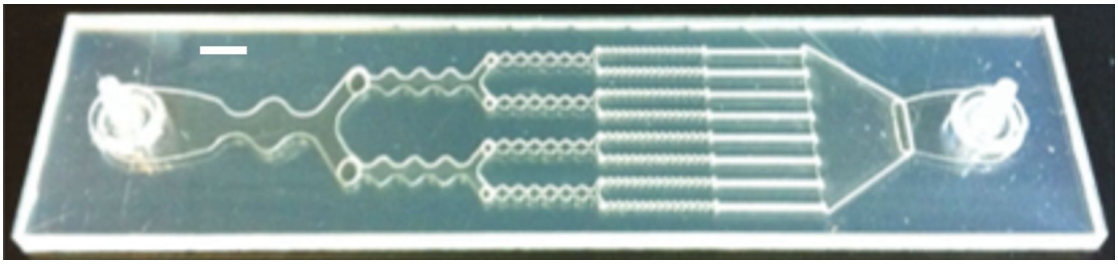

Figure 3. Microfluidic device for dissociation of tumor aggregates. The tumor aggregates are placed in the device on the left hand side and pass through the channels to the right due to forces created from water flow. Features were laser etched into layers and simulations were performed at 1 mL/min. Scale bar: 5mm.

Another novel microfluidic device is shown below and was used to dissociate brain tissue into single neurons [7]. Once again, this device was created to surpass the uncertainty and non-standard protocols of pipetting and mixing that were used previously. Their solution was to create a device with a single small channel in the center (Figure 4). The researchers used two syringe pumps that were programmed to create an oscillating fluid flow that forced the tissue back and forth through the device to induce shear stress and force cells to enter this small channel. It successfully dissociated neurons. The device was fabricated using PDMS and pressed between pieces of acrylic to seal.

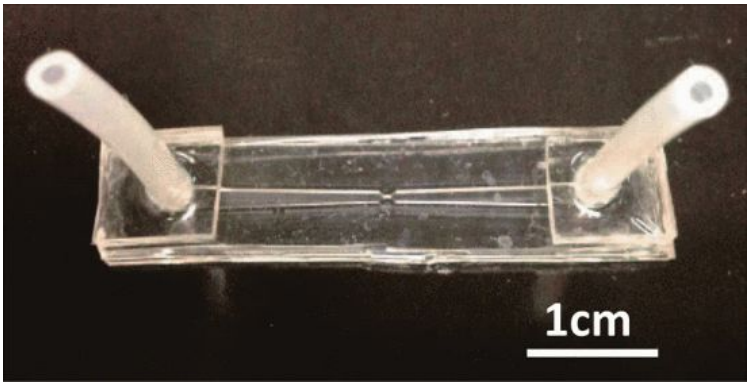

Figure 4. Microfluidic device for dissociation of neurons. Oscillating fluid flow is pushed through the tubes on either end of the device to the small channel in the center in order to dissociate neurons from the tissue.

Problem Statement

Dr. Mathur's asthma research requires biopsies of lung tissue before and after an induced asthmatic reaction. The tissue needs to be dissociated so that changes in the cells can be studied using flow cytometry. The biopsy size that needs to be dissociated is about 12 mm^3. The team was told that this small tissue sample is unable to be dissociated with the current dissociation methods. Therefore, the team is tasked with creating a dissociation device that will successfully dissociate a smaller tissue sample and yield at least 10,000 viable cells to study.

II. Background

Relevant Biology

The purpose of the device is to successfully dissociate lung biopsy tissues for asthma research. Though there are different causes of asthma, the client focuses on allergic asthma. In allergic asthma, harmless airborne allergens trigger an inflammatory response in airways of the lungs, called bronchial tubes. This response is initiated when mast cells release large amounts of histamine to flood the area with extracellular fluid, which attracts eosinophils and neutrophils to the affected site (Figure 5). Eosinophils contain granules with bactericidal, and virucidal proteins that can also damage native cells and cause the infiltration of more immune system cells [8]. Other cell types are also involved in the inflammatory process, but studies with new drug classes that reduce eosinophil activity greatly reduce the asthmatic response, which demonstrates that these are the main regulator of asthma activity. Eosinophils, besides inciting inflammatory cytokine cascades, also promote fibrosis and extracellular matrix remodeling which causes excessive repair in the lung tissue [9]. Because of eosinophils' role in asthma, it is the focus of most asthma research. Eosinophils are normally present in the blood at very low concentrations, and as a result have always been very difficult for researchers to obtain a sufficient number for study. However, since blood is easier to access and eosinophils can be filtered from blood fairly

quickly, it is the main media used for the study of eosinophils in asthma research. Recent studies have shown that there is great variability in eosinophil count using peripheral blood which has led researchers, such as our client, to believe that this method is not the best biomarker to use for asthma [10]. This is a major reason why lung tissue biopsies are necessary to more accurately studying the disease.

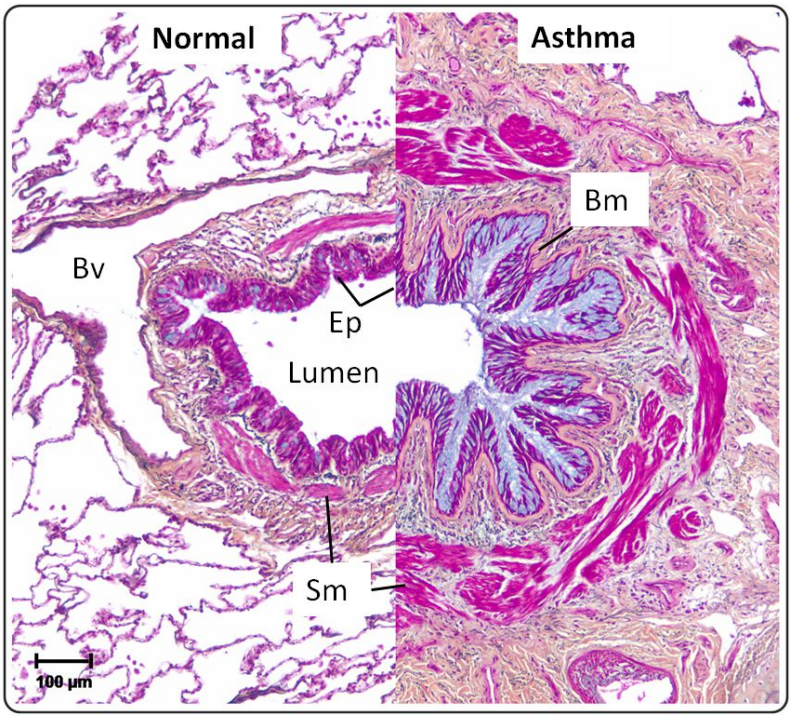

Figure 5. Asthmatic Bronchial Tissue**.** This image depicts the cellular level reaction of asthma in a bronchial tube cross section. In comparison to normal tissue, inflammation is clearly present in the asthmatic tissue. Bv, blood vessels; Sm, smooth muscle; Bm, basement membrane; Ep, epithelium [11]

To analyze changes in the lung tissue with the allergic response, a biopsy must be performed. There are several biopsy procedures to collect the tissue sample: open, needle, thoracoscopic, and transbronchial. The open biopsy is completed by making an incision in the chest to surgically remove tissue. Similarly, the needle process involves guiding a needle through the chest wall with a CT scan or fluoroscopy.

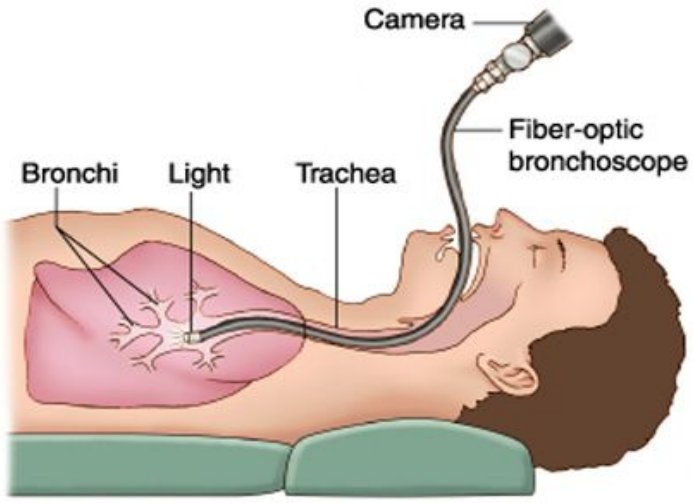

Figure 6. An example of bronchoscopy, a method used by the client to remove pieces of lung tissue for cellular analysis [12].

Thoracoscopic biopsies push an endoscope into the chest cavity, and then through the endoscope tools can be inserted to obtain tissue. Nodule removal or tissue lesion may also be performed. Lastly, the transbronchial biopsy, or bronchoscopy, guides a fiberoptic bronchoscope through the nose and into the bronchioles, where the device removes a ~12 mm^3 sample of tissue [15]. These techniques vary in invasiveness, with some requiring anesthesia. The lung biopsy procedure the client uses is the bronchoscopy (Figure 6).

Once the tissue sample is obtained, it must be dissociated into individual cells. Dissociation is the process by which single cells are liberated from a cell aggregate. To achieve this, the extracellular matrix (ECM) must be broken apart without lysing the cells themselves. Two main ways of dissociation include mechanically applying shear forces to the tissue and enzymatically breaking down the extracellular matrix. Unfortunately, many methods of mechanical and chemical dissociation disturb surface markers, nullifying data received from flow cytometry.

Flow cytometry is a method for analyzing the expression of molecules on the cell membrane and within the cell. These cells are fluorescently tagged for specific proteins and ligands on their surface using immunocytochemistry. This fluorescent intensity is then measured by the cytometer (Figure 7). The device has lasers that focus on single stained cells at a time and measure the light scattered and fluorescence emitted [16]. One particular measurement the client desires is the ability to analyze is the activity of eosinophils. Eosinophils are a type of white blood cell, and normally account for only 5% of all white blood cells. High eosinophil counts are related to asthma and allergies, and flow cytometry can detect the amount of these cells.

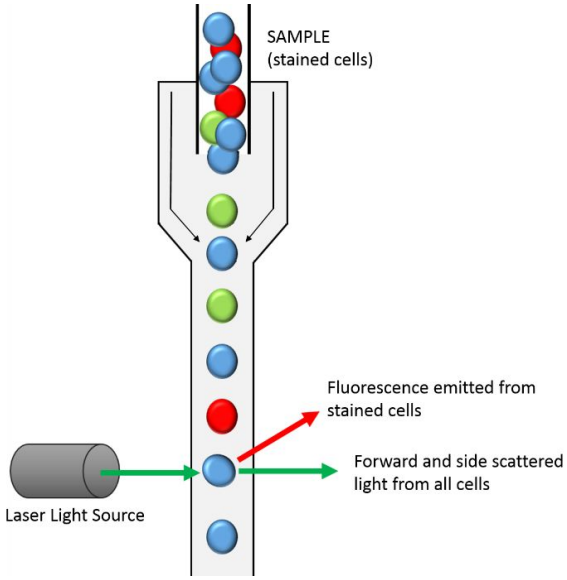

Figure 7. A flow cytometer measures the fluorescence of stained cells and sorts these cells based on fluorescent markers to allow for very specific measurement of the number and types of cells in a mixture [17].

When dissociating cells it is important to know the amount of cells expected to be in the tissue to know if the device is yielding the amount you want. There are some ways to test a device that will allow for the quantification of cells that make it through which is detailed later. Here we want to look at quantifying the amount of cells that can be obtained from lung tissue biopsies. Since testing is performed on both murine and human models, we look at both counting mouse and human cells in lung tissues. One study conducted found that the average lung volume was 8.6 cm^3 with 86.8% of it being alveolar region and 7.25 x 10^8 number of cells in that region [18]. Back calculating, this means there are 9.72 x 10^7 cells per 1 cm^3 of tissue. Our tissue is approximately 12 mm^3, which means there are approximately 1,200,000 cells in a mouse sample of that size. This cell count is composed of all types of cells. A similar study looked at the cell count in a human lung [19]. It was found that there are on average 230 x 10^9 cells per 4,341 mL of lung tissue. This translates to 5.29 x 10^7 cells per 1 cm^3 of tissue. Once again, assuming our sample size is 12 mm^3, there are approximately 600,000 cells.

Since the premise of the device being developed is that shear stresses created using fluid flow in small channels will dissociate cells from the extracellular matrix, it is important to look at how large we want to make the forces. A big benefit of microfluidic devices is that large forces can be created due to small channel sizes and high fluid velocities. In tissues such as heart valves, cells must withstand high shear stresses over a lifetime. They experience a peak shear stress of 7.7-9.2 Pa each time the heart beats. The cells can obviously not detach from the tissue each time they are exerted to such stress [20]. However, this cannot be the sole basis of our force analysis since lung tissue is not exposed to the same type of stresses since there is no constant fluid flow over the majority of the tissue. Another study used a microfluidic device to look at

shear stresses required to disrupt cell adhesion on a glass surface. What this group found is that even at stresses greater than 16 Pa, cell were still adhering to the surface of the device after extended periods of time [21]. Once again, this is not a good model of lung tissue dissociation since these cells are flattened out and adhered to the surface of glass rather than embedded in extracellular matrix. The most accurate model of shear stresses is probably the tumor aggregate dissociation device, which successfully utilized a shear stress of 0.9 Pa to dissociate their tissue[6].

Product Design Specifications

The main specification for this project is the development of a device to successfully dissociate lung biopsy tissue samples which are ~12 mm^3 in size. There must be a minimum of 10,000 cells recovered with the cells being ideally white blood cells. Since the dissociated tissue will eventually be run through a flow cytometer for analysis, there should be no disruption to cell characteristics such as eosinophils. The device's cost should not exceed approximately $10 per use, and if it is reusable, the material must be able to withstand sterilization procedures, either ethanol or autoclaving. A more complete list of design specifications can be found in Appendix A.

Previous Work

Last semester three members of the current design team worked to create a device that would dissociate cells from a lung biopsy sample. Three different design ideas were evaluated including a modification of the Miltenyi gentleMACS to fit smaller tissues, a microfluidic device with decreasing sized channels, and screw device that would use mechanical degradation to break apart the tissue. After evaluation, the team decided to pursue the microfluidic design. The design consisted of a single layer with channels that branched and got smaller to a final width of 0.6 mm. The team fabricated the device using the SLA 3D printers at the Makerspace. Four rounds of testing were conducted with the device but there were some difficulties with the flow rate and with the device not being sealed properly. The team was unable to get a tight seal with using a acrylic top and rubber o-ring last semester which resulted in leaking of the fluid and an inconsistent flow rate. The peristaltic pump that was used last semester to drive the sample through the device was only able to achieve a flow rate of 15 mL/min. Due to these problems the device failed and the tissue did not pass through the channels resulting in minimal cell recovery. It was believed that if the leaking problems were addressed, that the device would then dissociate cells from the lung tissue.

III. Preliminary Designs - Fabrication Methods

Since the proposed final design is very similar to the design of the previous semester, the team determined that an evaluation of various fabrication methods to improve usability and fluid flow would be helpful. The team researched several possible fabrication methods for creating smaller channel sizes for our device. The fabrication methods were narrowed down to four options: 3D printing, PDMS photolithography, laser cutting, and micromilling.

Fabrication Method 1 - 3D Printing

3D printing is a process that makes solid three dimensional objects from a converted digital file using different plastics. The process involves creating the general base outline of the intended object and adding layer by layer along the z-axis. The device fabricated last semester was made using an Ultimaker 3 at the UW-Madison Makerspace. This type of printer uses fused deposition modelling. This technique uses thermoplastics that are melted and extruded through the nozzle onto the stage in layers. This option was utilized last semester because it was cheap (<10$ per print at the Makerspace), quick, and available, but it had some drawbacks. Specifically, this printer has layer thickness of 250 microns. It also had support material in the channels which was hard to remove.

This semester, the team considered stereolithography (SLA) printing in order to achieve a better resolution for the design. SLA works by taking layers of photocurable liquid resin which are crosslinked using a UV laser [23]. Once this is complete, the product must cure, meaning it must be exposed to heat and UV light. On the UW-Madison campus, the best SLA printer available is the Viper 3D printer at the Morgridge Fab Lab (Figure 8). This printer can print layers as small as 20 microns. Robert Swader, a mechanical engineering within the Fab Lab, was consulted about using this method of 3D printing. He made a point that the materials used in SLA printing have cytotoxic effects due to the presence of methacrylate and acrylate, but very little is known about these effects [24]. He mentioned that researchers have tried curing their devices in an inert environment with some, but not measured, success. Some studies have been conducted with SLA materials. One study used DSM Watershed and found that if treated with ethanol after curing, zebrafish embryos could be cultured [25]. Another study cultured Chinese hamster ovary cells in a SLA printed device and found nearly identical growth curves when compared with regular tissue culture materials [26]. Further research must be done on the specific materials used on the Viper 3D printer and how they can be cured and treated to ensure biocompatibility.

Figure 8. Viper SLA 3D printer at Morgridge Fabrication Lab. Layers of resin are photocured into the 3D design, with a high precision laser.

Fabrication Method 2 - PDMS Photolithography

Polydimethylsiloxane, or PDMS, is an elastomeric polymer often used for fabrication of microfluidic devices. PDMS devices are fabricated using a very precise mold, and they are able to replicate features down to the nanoscale [27]. One of the most common methods to create a mold is via photolithography. This method involves the creation of a master, which is essentially the negative of the desired features within the PDMS device. Masters can be created from SU8, which is an epoxy based negative resist. This viscous material is applied to a silicon wafer and the desired thickness is attained by spinning the wafer at a particular RPM. The wafer is then treated with heat, covered with the desired template, and then crosslinked with UV light. Excess SU8 is washed away with a developing solution, leaving the master with the crosslinked features.

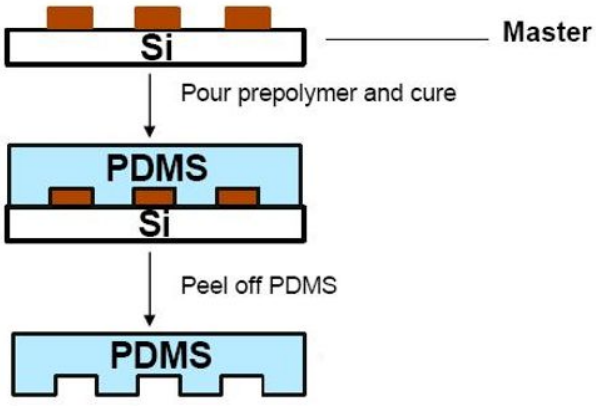

Figure 9. General process for soft photolithography. A master is created on a silicon (Si) wafer with the negative features of the desired device. Polydimethylsiloxane (PDMS) is poured over the top of the master and cured with heat. Once completed, the PDMS is peeled of the master and the device is ready for use.

In order to fabricate the PDMS microfluidic device, liquid PDMS and a curing agent are mixed together. The mixture is placed in a vacuum to eliminate all bubbles before pouring onto the master. This pour occurs on a hot plate and is left to heat for approximately 4 hours. Once the PDMS has fully cured, the microfluidic device is able to be peeled off of the master and is ready for use. This process is illustrated above in Figure 9.

The team considered PDMS photolithography for a variety of reasons. This method is very cost efficient and would allow us to stay within the goal of $10 or less per use. It is also well-known that PDMS is a biocompatible material, which is an important aspect in our design. The team has worked with this fabrication method before and the materials are readily available in the BME tissue lab. However, the drawback of this fabrication method is that the device would not be able to get as thick as the team desires. In order to get to the desired thickness, an alternative type of mold would need to be used. Micromilling is most often used to create thicker molds, which is in itself a fabrication method the team is considering.

Fabrication Method 3 - Laser Cutting

Laser cutting is a process that uses a high powered precise laser to cut a design from a vector file into the material by melting, burning, or vaporizing. Laser cutting requires a very good exhaust ventilation system in order for many materials to be used due to the fumes that are created during the cutting process. The laser width directly correlates with the accuracy of the device. The laser cutter that is available to the team for fabrication is the ILS9.150D which has a 10.6 micron $C0_2$ laser that operates at up to 150 watts (Figure 10). The device would be fabricated using many laser cut layers glued together. Unfortunately, the laser printer available at the UW-Madison Makerspace can only be used with organic materials, so the plastics we would like to used may not be available for us to cut.

Figure 10. ILS9.150D laser cutter. Has a cutting area of 24” x 36”, can cut most natural materials including paper, wood, and acrylic. It uses a 10.6 micron carbon dioxide laser. Available for use at the UW-Madison Makerspace.

Fabrication Method 4 - Micromilling

Milling is the process of using a rotating tool in a movable head to remove material from a product. It is a widely-used machining process and can be scaled down to the micro scale for use on biomedical research applications (Figure 11). It can be used by designing a 3D model on a CAD program and the translated into computer numerical controlled (CNC) tooling paths that automatically machine the piece into the material of choice. Micromilling uses end mill tooling that can reach sizes of less than 50 microns. This poses problems since machining exerts bending forces on these small bits and causes them to break at very small forces, so machining at any depth we would be limited to wider tooling or risk of frequent breakage.

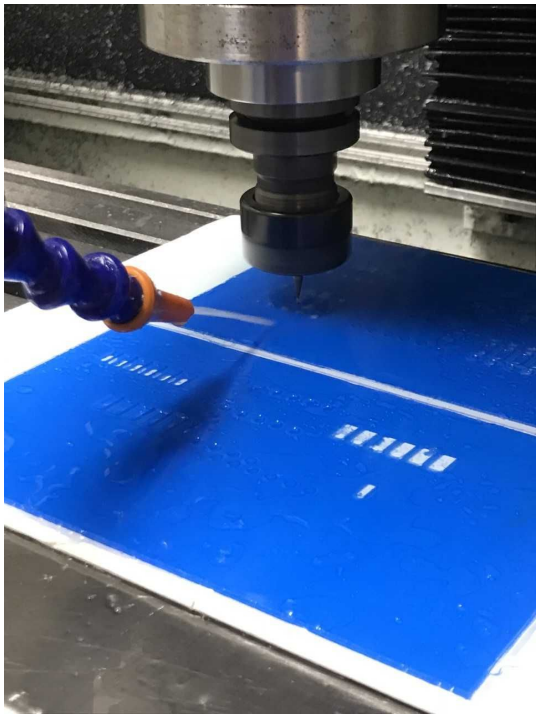

Figure 11. Micromilling with a 0.02 inch (diameter) drill bit into poly(methyl methacrylate). Micromills can machine almost any material including plastics and soft metals reliably. Difficulties include breaking the tooling and creating programs.

VI. Preliminary Design Evaluation

Design Matrix

The team created a design matrix comparing the four fabrication methods with the following criteria: accuracy, materials, ease of fabrication, and cost (Table 1). Accuracy was

defined as the ability of the fabrication method to produce a device with the desired geometric properties and resolution. This criteria also takes into account the ability of the device to successfully apply shear forces to the tissue. Accuracy was weighted the highest (35/100) because the device must be able to function and dissociate tissue or the device is essentially ineffective.

The materials category was defined as the compatibility of the fabrication method with certain materials of interest. Some of the fabrication methods required specific materials which were not autoclavable or may be cytotoxic. Therefore, this category was rated highly (30/100) to determine which fabrication method allows the use of the best material for this project (ideally non-cytotoxic, autoclavable, non-degradable, etc.)

Ease of fabrication was defined as the general effort that would be needed for the team to produce the prototype device (time, skill, safety, etc.). This category was rated third highest (20/100) because if the previous two criteria are not met then the device is not worth fabricating at all. However, ease of fabrication is very important because testing should begin as soon as possible, and if it takes half of the semester to make the device, then little time is left to prove its efficacy. Also, once the team is done with producing a prototype device, the client would ideally be able to create further devices independently if given proper direction.

The final category, cost, was defined as the total cost of fabrication method, including various materials (device material, end mill bits, Makerspace fees, Morgridge Fab Lab fees, etc.). The cost of the fabrication itself is not of utmost concern of the team, therefore it was given a lower rating (15/100). Because the final device needs to cost less than $10 per use, materials must be chosen carefully.

Table 1. Preliminary Design Matrix - Fabrication Methods. The light green shading indicates the fabrication method was the highest score for each criterion. The dark greed shading indicates the highest overall score comparing the four different methods.

Criteria	3D Printing	PDMS Photolithography	Laser Cutting	Micromilling
Accuracy (35)	28 (4/5)	21 (3/5)	21 (3/5)	35 (5/5)
Materials (30)	18 (3/5)	30 (5/5)	24 (4/5)	30 (5/5)
Ease of Fabrication (20)	20 (5/5)	12 (3/5)	12 (3/5)	8 (2/5)
Cost (15)	12 (4/5)	12 (4/5)	15 (5/5)	3 (1/5)
Total (100)	78	75	72	76

Accuracy: Micromilling was rated highest because the bits can get extremely small and thus, practically any size channel could theoretically be fabricated. 3D printing was ranked next because it has a resolution of about 150 um. Laser cutting was rated 3/5 because the nozzle is cone shaped, so the channels would be wider on the top than the bottom. And finally, PDMS was also rated 3/5 because it wouldn't be easy (or possible) to make the master as thick as is needed (0.5 mm) to fit the tissue samples.

Materials: Micromilling also scored the highest in this category because nearly any material can be micromilled. PDMS scored full points in this category as well because PDMS is a known biocompatible material that shouldn't disrupt the cell markers in any way. Laser cutting and 3D printing scored lower because materials are more limited, and in the case of 3D printing, the biocompatibility of the material has not been fully investigated.

Ease of Fabrication: 3D printing scored the highest in this category because the team is most familiar with this method and it would be the fastest. The other designs scored lower because they would take more work and time (especially micromilling).

Cost: Laser cutting scored the highest category because essentially the only cost would be the raw material. PDMS and 3D printing scored equally because they are fairly cheap. Micromilling scored the lowest because many expensive bits will be needed to produce the design.

While all three fabrication methods are fairly close in terms of how they score, 3D printing is the best option for this semester. It scored highly in our two most important categories, accuracy and materials, and the team is most familiar with this method. 3D printing will allow the team to spend more time on testing for a proof of concept, rather than learning a new fabrication method. While it did not receive perfect scores in the two most important categories, the accuracy from 3D printing should be sufficient to make a proof of concept prototype. Secondly, it was rated 3/5 on materials because the materials that can be printed have not been thoroughly investigated for their cytotoxicity. However, the tissue sample will not be exposed to the material for very long, and cytotoxicity testing will be implemented by 3D printing a culture shaped dish with the material and culturing epithelial cells and eosinophils in order to establish if there are any detrimental effects on the cells.

Final Design

The final design is based off of the design from last semester, but is mirrored at the narrow channels so there can be flow alternating back and forth within the device. Another set of narrower channels was added to this device (Figure 12). One of the reasons the design didn't work last semester was due to issues with keeping the device watertight. This semester, a rubber gasket was used, as well as a thicker acrylic cover to allow for more uniform sealing.

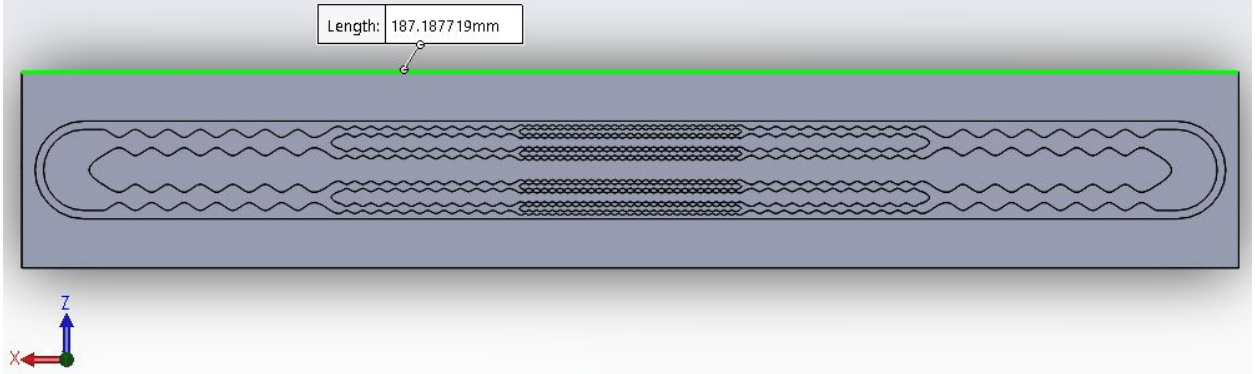

Figure 12. Final design with length shown. The channel minimum thicknesses from left to right are 1.6 mm, 0.64 mm, and 0.3 mm in the middle, and then mirrored about the center. The long pill shaped region surrounding the channels is an inlay for a rubber gasket.

V. Fabrication

Materials

The final decision for the fabrication process was 3D printing using the SLA printer at the Morgridge Fab Lab. The material that was used to print our design will be Accura 60 from 3D Systems. This is because there are only two material options available at the Fab Lab and our consult suggested the use of Accura 60 as the less cytotoxic material. The cost of the print was $35.00 (Appendix D). We utilized the Morgridge Fab Lab laser cutter to fabricate four silicone gaskets for free. Other materials utilized include a handmade rubber gasket, an acrylic cover piece, and three bar clamps. These items were obtained for free from the UW-Madison TEAM Lab.

Methods

The final design was modeled in Solidworks and sent to the Morgridge Fab Lab to be printed on their 3D Systems Viper SLA printer. The silicon gaskets were also cut at the Fab Lab to fit the dimensions of the Solidworks model of the device. The ends of the device were modified to allow the incorporation of input/output adaptors. A protocol for assembling the device for testing has been written. These protocols can be found in Appendix B.

Final Prototype

The final prototype was fabricated by methods detailed above. The prototype system used for testing can be seen in figure 13. It has the 3D printed device connected by peristaltic pump tubes at each end. In the groove, a silicone gasket is placed. Since the only available silicone to laser cut was very thin, another thicker silicone piece was placed on top. Next, an acrylic piece of about 0.5 in. thick was put on top of both silicone pieces. This whole system was then clamped to a table using 3 Quick-Grip clamps.

Figure 13. (Left) The 3D printed device is connected to the input and output tubing and silicone gasket placed within the indentation. (Middle) The handmade rubber sheet and acrylic cover are placed over the silicone gasket. (Right) The acrylic cover is clamped to the device with 3 bar clamps.

VI. Testing

This semester the team wanted to address the hypothesis that our device is able to dissociate more than 10,000 cells per tissue sample and that it is able to outperform the current device used by the client, the Miltenyi GentleMACS.

Modeling Fluid Flow

We modeled the final design for fluid flow with the Solidworks Flow Simulation Toolbox. The input volumetric flow rate of .24 mL/s and output environmental pressure initial conditions were set, as well as the computational domain. The project was run and analyzed for

velocity profiles, pressure profiles, and wall shear forces throughout the device, we found a maximum velocity of about 0.1 m/s in the smallest channel, and a maximum shear force of about 1.28 Pa also in the small channel.

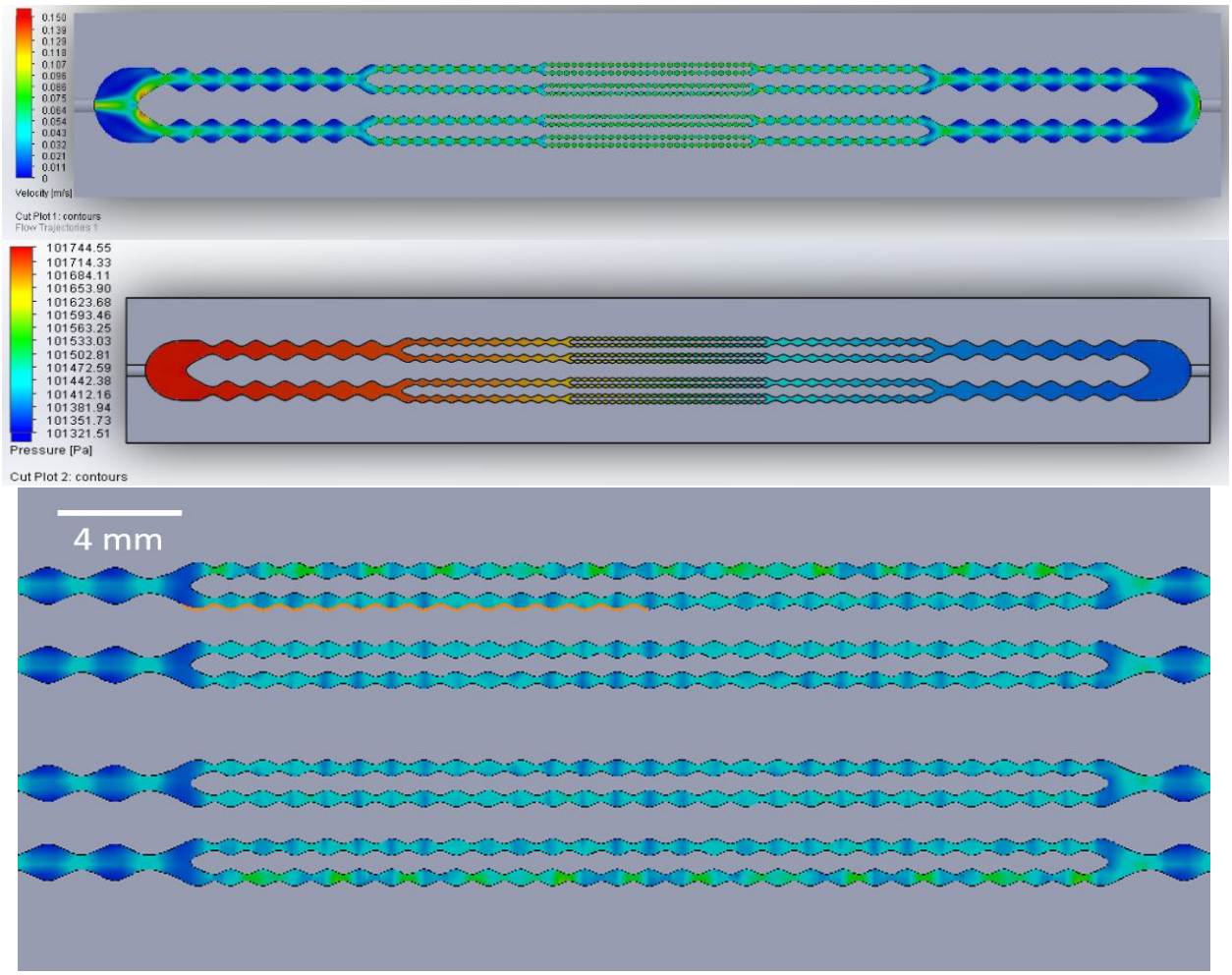

Figure 14. Results of Solidworks simulation. (Top) Velocity profile through device showing a maximum velocity of about 0.1 m/s in the smallest channels in the center. (Middle) Pressure drop through device. Largest drop is through smallest channels as expected. (Bottom) Close-up of wall shear forces in the smallest channels, these forces were found to be a maximum in green at ~1.28 Pa. Scale bar 4 mm.

Preliminary Testing

After printing the final design and laser cutting a rubber gasket, multiple rounds of preliminary testing were conducted to solve the problem of the device leaking. As indicated in the final prototype, the leaking was solved by using the rubber gasket in conjunction with another piece of rubber cut to fit the device, then sealing the whole device by clamping an acrylic lid on top.

Other preliminary testing that was conducted used approximately 100,000 human epithelial cells that were counted before and after being sent through the device. This testing

allowed us to examine the retention rate of cells being passed through our device to be sure that no cells were attaching to or getting stuck in the device.

Variable Studies

There were a number of variables the team believed could lead to changes in the number of cells retrieved from the sample in our device, namely filtering before centrifugation vs. not filtering, low vs. high flow rate, and fresh vs. frozen tissue.

We first examined the use of filtering with a 50 micron filter after dissociation with our device vs not filtering. The team observed a bigger pellet after centrifugation and a much higher cell count when no filtering was used. The initial thought to not filter the dissociated cells was to help any loose cells left on the sample after passing through the device be removed from the sample.

We also tested the variable of flow rate by using a different peristaltic pump that could generate a higher and more consistent flow rate. The flow rates for each of these pumps (the clients vs. then newer pump from the Tissue Lab) was calculated by setting the pumps at their maximum value and running a measured amount of water through the pump and timing the amount of time it took for all the water to run. From this calculation we found that the older pump had a maximum flow rate of 15 mL/min where the newer peristaltic pump had a maximum flow rate of 30 mL/min. We compared the effect that the different flow rates had on the average cell count obtained by using frozen mouse tissue samples and our new device to dissociate the samples.

The other major variable we wanted to examine was the use of fresh murine lung tissue versus using frozen murine lung tissue. The frozen mouse tissue was much more accessible for the team than the fresh tissue which played a major factor in testing our design. We were able to assess the difference in average cell count from dissociation using fresh tissue versus frozen tissue. This test was conducted using the older peristaltic pump.

Final Testing

The major comparison we addressed in our testing was how our device compared to Miltenyi GentleMACS™ and to see if we were able to successfully dissociate enough cells to satisfy our design requirements. In order to rule out any differences in sizes of the tissue biopsy samples we were able to normalize our cell count from dissociation to the size of the sample used. We were able to calculate the volume of the tissue samples by using ImageJ (Appendix B, Appendix E). The samples were then labeled and randomly sorted into three categories, dissociation with the device, dissociation with the device with no filtering, and dissociation using the Miltenyi GentleMACS, figure 15.

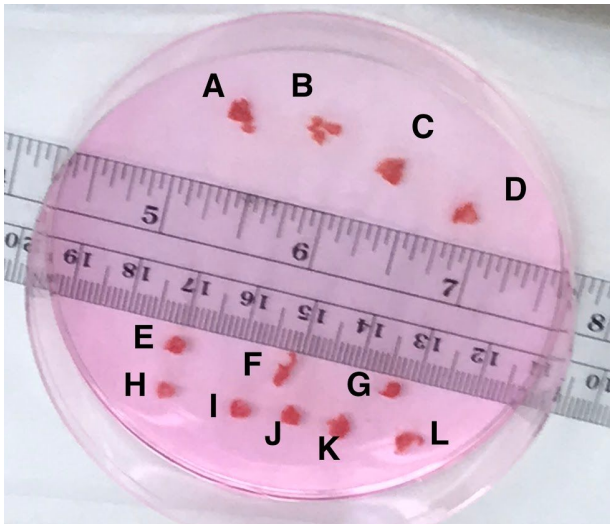

Figure 15. Biopsy samples that were taken from frozen murine lung tissue and placed in media (DMEM). A ruler was included in the picture to allow for ImageJ analysis. Samples were labeled to record cells per mm^3 after dissociation. Samples A-E were used in the device with filtering, F and G were used with the device with filtering, and samples H-L were used in the Miltenyi GentleMACs.

The same general lab procedure that our client has been using for their tissue dissociation was used throughout testing (see Appendix B) with modifications for specific tests. Samples were incubated in the collagenase solution provided by Miltenyi and then placed in the device, figure 16. The device is then sealed using the silicon and rubber gasket, acrylic lid, and the three clamps. The tubing is hooked up to the peristaltic pump and the device and the liquid and the sample is ran through the device two times. Afterwards all the liquid is collected in a conical tube and if the tissue sample is still in the device it is manually removed and placed in the liquid. This is then either strained with a 50 micron filter, or not depending on testing group, and centrifuged. The supernatant is then removed and the pellet is resuspended.

Figure 16. (Left) Biopsy samples that were taken from frozen murine lung tissue and placed in collagenase solution and incubated for 45 minutes at 37℃ . **(Right)** The biopsy sample is removed after incubation and placed into the device via pipette with approximately 300 µL of the collagenase/PBS solution.

For each tissue sample 20 µL was taken from the resuspended pellet and was mixed with the buffer for the cell counter. This was then placed in the cell counter and measured three times, recording the measurements for the parameters of 4-7 µm, and for above 4µm, figure 17.

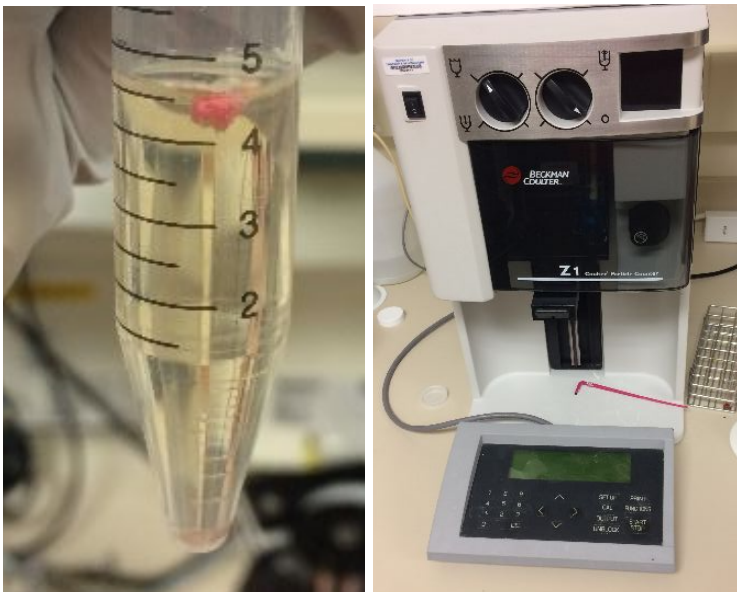

Figure 17. (Left) Biopsy samples after centrifugation in the collagenase solution with no filtration, a visible pellet is seen in the bottom of the conical tube. **(Right)** The beckman cell counter was used for obtaining the average cell count of the dissociated tissue samples.

VII. Results

Preliminary Testing

The results of initial testing showed that the device did not trap any cells that went through it, and the cells did not adhere to the device. Approximately 210,000 cells/mL were sent through the device, and approximately 300,000 cells/mL were measured coming out of the device. While this second count shouldn't be higher, we believe that this is due to error in the particle counting machine.

Variable Studies

The data collected during testing was sorted based on three variables that could affect how the microfluidic device works including fresh or frozen tissue, older peristaltic pump versus newer, and straining versus unstraining. The direct comparisons between these groups was

determined using a two-sample independent t-test which allows a direct comparison between the means of two sample groups to determine a significance. Significance was assessed as $p < 0.05$.

The first comparison that was analyzed was the use of the straining method with the 50 micron filter after dissociation versus not straining the dissociated solution, figure 18. The average cell count was determined by taking the average of all the readings from the cell counter (4-7 µm) for all the samples in the straining and no straining category. As shown in figure 18 there is a significance difference in average cell count when straining the dissociated cells compared to not straining, p-value 0.005 and the average cell count for the without straining was approximately double the cell count for the with straining group. There was a four times greater variance observed in the without straining group compared to the with straining group.

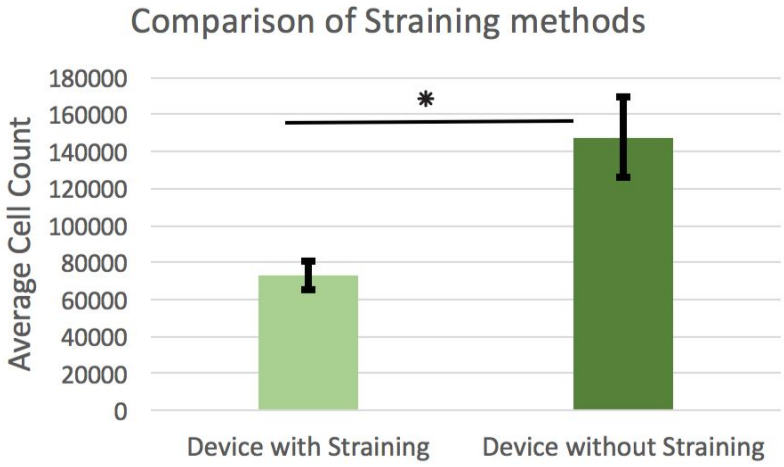

Figure 18. Comparison between using the staining method with a 50 micron filter compared to not straining the dissociated cells. Only frozen tissue and the newer pump was used for this comparison. Bars depict average cell counts and error bars depict SEM. Straining AVE=7.28E+04, SEM=8.00E+03, n=7. Without straining AVE=1.47E+05, SEM=2.14E+04, n=5. T-test p-value = 0.0005.

Another comparison that was analyzed through testing was the older peristaltic pump versus the newer peristaltic pump, figure 19. The average cell count was determined from taking the average of the all the readings from the cell counter (4-7 µm) for all the samples in the category. As shown in figure 19 there was a significant difference in average cell count, p-value 0.015, when using the old pump compared to the new pump with almost double the average cell count in the new pump compared to the old pump. There was a three times greater variance in cell count when using the new pump compared to the old pump.

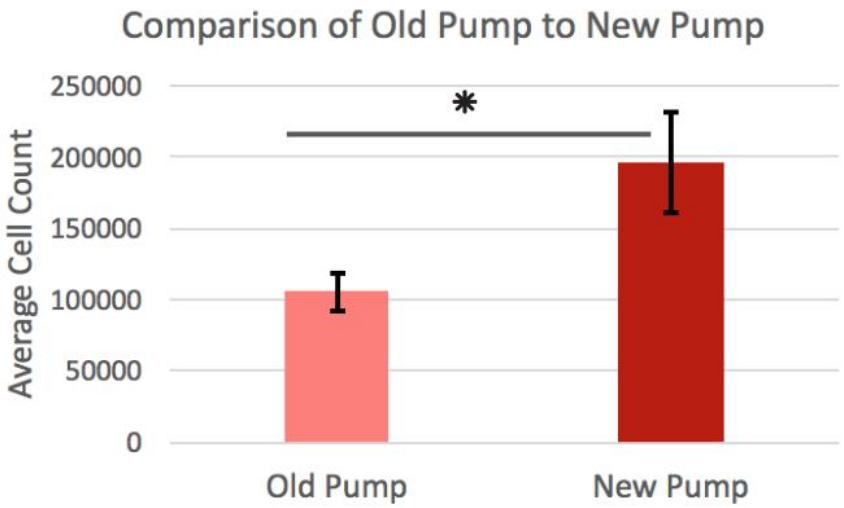

Figure 19. Comparison between older and newer peristaltic pump. Only frozen tissue was used for this comparison. The older pump yielded a maximum flow rate of 15 mL/min compared to 30 mL/min for the newer pump. Bars depict average cell counts and error bars depict SEM. Old pump AVE=1.05E+05, SEM=1.30E+04, n=3. New pump AVE=1.96E+05, SEM=3.5E+04, n=12. T-test p-value = 0.015.

The next comparison that was analyzed was the difference in average cell count when using frozen mouse lung tissue compared to fresh mouse lung tissue, figure 20. The average cell count was once again determined by taking the average of all the readings from the cell counter (4-7 µm) for the samples in this category. As shown in figure 20 there was a significant difference in the average cell count when using fresh tissue versus frozen tissue with the fresh tissue, p-value 0.0004, having an average cell count that was approximately three times greater than the frozen tissue average. The variance for the fresh tissue was five times greater than the frozen tissue.

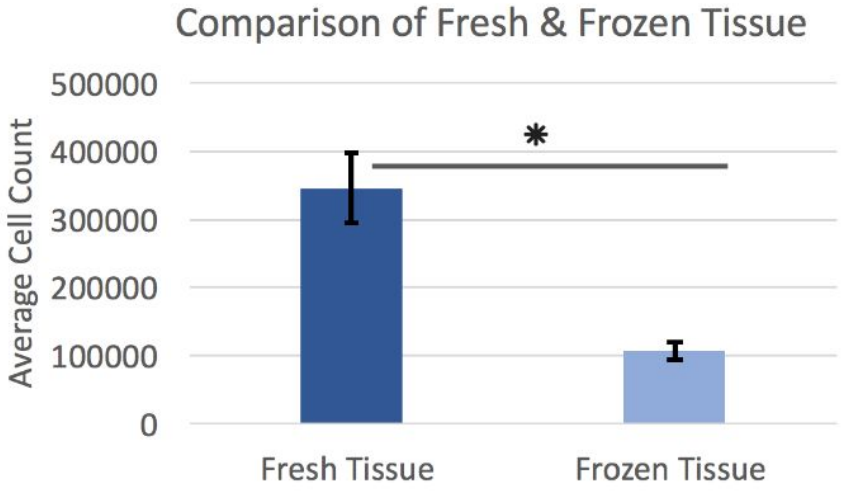

Figure 20. Analysis of fresh tissue samples compared to frozen tissue during dissociation with our device. All samples were filtered and dissociated using the old peristaltic pump. Error bars depict SEM. Fresh tissue AVE=3.46E+05, SEM=5.08E+04, n=2. Frozen tissue AVE=1.05E+04, SEM=1.30E+04, n=3. T-test p-value = 0.0004.

Final Testing

The main variable tested in the final round of testing was the cell counts using the device or the gentleMACS dissociator. For this testing, three separate groups were analyzed, the microfluidic device with straining, the microfluidic device without straining, and the gentleMACS dissociator with straining. The average cell count was normalized using the tissue sample volume so that the final reported data was cells/mm^3. A single factor ANOVA was used when comparing three different groups to assess difference between the means.

Figure 20 shows the results of the three groups. Namely that both gentleMACS and the device without straining performed statistically significantly better than the device with straining. Interestingly the device without straining performed almost the same as the gentleMACS with a p-value of .95. One interesting observation was that the device with straining was much more consistent than the gentleMACS, while all readings for the device without straining fell between 17,000 and 21,000, the Miltenyi device had a range of 10,000-30,000 with most readings falling below 16,000. The microfluidic device seemed much more specific which can be seen in the standard error.

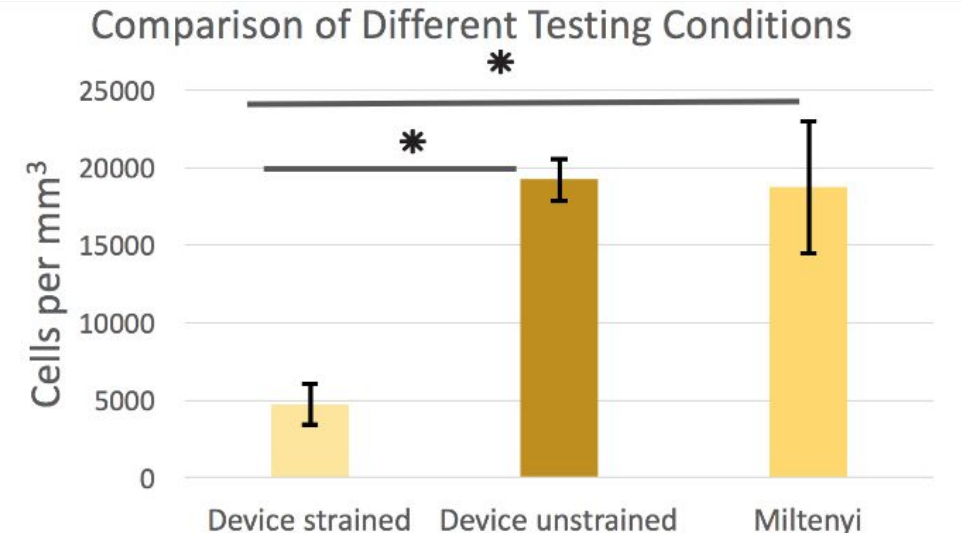

Figure 21. Testing conditions were analyzed by comparing the average number of dissociated cells per mm^3 of tissue. Tissue volume was measured using ImageJ. All samples were frozen and used with the newer peristaltic pump. Error bars depict SEM. Device strained AVE=4.76E+03, SEM=1.3E+03, n=5. Device unstrained AVE=1.91E+04, SEM=1.3E+03, n=2. Miltenyi AVE=1.87E+04, SEM=4.24E+03, n=5. ANOVA yielded p-value = 0.01 between groups. T-test between device strained and device unstrained p-value = 0.0015. T-test between device strained and Miltenyi p-value = 0.013. T-test between device strained and Miltenyi p-value = 0.95.

IX. Discussion

Modeling Fluid Flow

The results of modeling the fluid flow through the microfluidic device in Solidworks show that the shear forces that the cells will be exposed to are slightly more than what they would experience in an arteriole [28]. We expected this flow to be fast enough to dissociate the tissue, but not lyse the cells, this value was also similar to what was used in the previous microfluidic device for dissociating cancer cells [6]. The flow simulation done in Solidworks did not quite come out as we expect, as velocity in the smallest channels was similar to the velocity in the constrictions of the larger channels, as such we would like to do the modeling in COMSOL multiphysics if we can.

Preliminary Testing

For the test consisting of regular plated cells being run through the device, the number of cells/mL was counted both prior to running them through the device, then counted again after coming out of the device. These values were approximately the same, indicating that when cells are run through the device they experience no adhesion to the surface of the device. This allows us to conclude that when cells are being dissociated away from tissue within the device, they will not adhere to the surface of the device and should be able to flow through the channels, out of the device, and into the collection tube. This testing also revealed that we are not losing any cells in the tubing used with the peristaltic pump.

Variable Studies

The three variables tested in these studies were fresh vs. frozen tissue, fast vs. slow flow, and filtering vs. not filtering. The results of these show that fresh tissue yielded significantly more cells than frozen tissue, which was expected because the client told us cells tend to be looser in fresh tissue vs. frozen tissue. Also with frozen tissue, it is possible that many cells were killed in the process of thawing and unthawing. With these results, we can say that further testing with frozen tissue should yield suitable cell count results. If we can get an appropriate number of cells dissociated from frozen tissue, then it is safe to assume there will also be a suitable number of cells dissociated from a fresh tissue sample.

With the fast vs. slow pump, we saw much more dissociation with the greater volumetric flow. Since the greater volumetric flow means higher fluid velocity in the channels, and thus more shear stress(shown by our calculations in Appendix E), then the results of this study support the proposed mechanism of dissociation by shear stress caused by fluid flow in the microfluidic channels.

Finally, there was a much higher average cell count when the cells collected from the device were centrifuged with the remaining small tissue compared to when the small tissue was

strained out with a 50 μm filter. It is unclear exactly why this is but it is expected that the centrifugation might further release loose cells from the tissue. However, it is possible that without straining, the particle counter is detecting pieces of ECM from the tissue which leads to a inaccurate cell count.

Final Testing

The final round of testing compared three conditions: the device with tissue strained, the device with tissue unstrained, and the Miltenyi with tissue strained. The results from this testing round allows us to make a few conclusions about these conditions. First, the statistical significance between the device strained and device unstrained conditions allows us to conclude that the device unstrained condition performed significantly better than the device strained condition. We saw a consistently higher cell count when the tissue was centrifuged with the collected fluid for reasons explained previously.The statistical significance between the device strained and the Miltenyi strained conditions also allows us to conclude that the Miltenyi performed significantly better than the device when tissue was strained prior to centrifugation. Finally, there was no statistical significance between the device unstrained and the miltenyi conditions. This allows us to conclude that our device, when the tissue is centrifuged with the fluid, performs at the same level as the device currently on the market. We also saw more consistent results with the device unstrained condition, whereas there was more variation with the Miltenyi condition.

It was unexpected that the Miltenyi would yield over 10,000 cells from a lung tissue biopsy of testing size. The initial motivation for the project was that this current device does not yield the appropriate amount of cells for flow cytometry. However, during our testing we found that the Miltenyi performs well above the client-given benchmark of 10,000 cells. Therefore, we can conclude that our device as well as the current device meet the design specifications but future characterization of the cells from both of these devices will help determine which does a better job. New metrics will need to be set to determine what a better cell population from the dissociated cells is necessary for testing.

Final Design Analysis

This section is intended to compare the overarching features of the final design against our design criteria and previous designs. We identified several successful design features. Our device has been shown to reusable, sterilizable, and low cost. We used the device over 15 times, we were able to sterilize the device each time, and the cost-per-use was less than $2. We have developed a repeatable dissociation protocol through iterative testing. This protocol can be easily followed by any laboratory technician familiar with working with tissue samples. We achieved a consistent dissociation of each sample into more 10,000 cells, fulfilling our design criteria. Virtually no leaking was observed in the final round of testing. Lastly, because the device

assembly is easily taken apart, any undissociated tissue can be retrieved easily after dissociation. This is important because it allows the sample to studied further by the researchers, it allows for the sample to be included in centrifugation, and it means that the sample can be re-run through the device.

We also found several improvements to the final design. First, we printed the device to be mirrored to allow for multidirectional flow, but we did not utilize this feature during the testing this semester. The method used to seal the device (clamping) was unwieldy and took up a lot of space. This process also required utilizing the edge of a lab bench, which may increase the probability that an accidental spill or drop will fall to the floor, causing more of a danger than if contained to the lab bench. Also, this method of sealing the device was not totally foolproof; we had leakage of fluid up until our final testing. It was never confirmed that the shear stresses present in the computer modelling are present in the physical device at the correct intensity.

X. Conclusions

Future Work

There were several design features we were not able to examine this semester. The first of which is is the oscillating flow using a programmable peristaltic pump. The peristaltic pump will be programmed and controlled via an Arduino (see Appendix C for code and circuit set up). In brief, the arduino was connected to an RJ-45 (ethernet) adaptor and plugged into the pump. Simple text commands are sent to the pump with a delay, and the pump will respond to those commands. While the pump itself has been tested for pure operation, it has not been tested with any fluid or with the device itself. Since the device has a mirroried design built specifically to accommodate this function, it should be implemented in future testing.

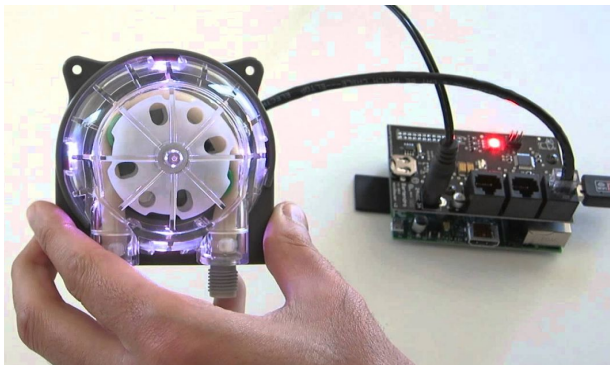

Figure 21. Programmable peristaltic pump connected to the suppliers routerboard (not used), Arduino used to power and control pump action, hand for scale. Inlets and outlets are underneath the hand in this photo.

Another flow design feature that should be more thoroughly tested is the amount of time the tissue spends in the device with fluid running over it. In the scope of this study, the tissue spent less than 1 min. with shear stress due to fluid flow in the device. Other devices used times

of 4 min. or ran fluid through the device 10 times, which suggests we should experiment with how many times fluid is run through our device before removing the tissue and centrifuging. Also, with the device itself, there should be a more thorough analysis of fluid velocity and shear stress within the device to inform any new design changes.

As mentioned above, the clamps used to seal the device were not the most functional, so it would be an improvement to instead widen the device and put screws through the acrylic that can be finger-tightened to seal the device. This would also necessitate printing or fabricating a new device that has minimal warping to reduce the forces necessary to seal the device.

A major limitation of the testing was accessibility to fresh tissue. Results show that more cells are dissociated from fresh tissue than frozen, so ideally any future testing will utilize fresh tissue. Frozen tissue also proved to be an issue when we tried to characterize the cells after counting. Once they were spun down, the cells were put on cytospins slides, but did not remain intact during the process which is thought to be because of the frozen tissue. Characterizing the cells once they are dissociated is incredibly important and the ultimate goal. In future testing, cells will be stained using HEMA3 to assess cell structure and type. Cytotoxicity tests will also be performed to assess cell viability after dissociation. Once murine tissue has been thoroughly understood, human tissue will be necessary to validate the device. Since the final goal is to assess the cells using flow cytometry, tests using flow will need to be performed.

Final Conclusions

The use of tissue biopsies is an important tool in the field of asthma research, especially in the careful study of eosinophilia. Tissue dissociation is used to gather individual cells to analyze the cellular makeup of the tissues via flow cytometry. The client, Dr. Sameer Mathur, supplied the team with the task to create a device that would allow his lab to dissociate tissues of 12 mm^3. After analysis of design specifications the team was able to develop a microfluidic design to fit the criteria and choose the method of 3D printing as the most suitable way to fabricate. The microfluidic device utilizes a set of diminishing channels with smooth constrictions as well as fluid flow using a peristaltic pump to induce shear stresses over tissue samples that are in solution. After testing, it was determined that this device, as well as the current device in the lab, both yield a suitable number of cells according to the client specification of greater than 10,000 cells. Future work will focus on testing oscillating flow within the device to keep the tissue under shear stress for longer. It should also focus on using fresh tissue and characterizing the cells once they have been dissociated. In a broader scope, once the design has been thoroughly tested with lung tissue, it may become applicable to other tissue types allowing for mechanical dissociation of several cell types that can be used in other fields of study to improve cellular analysis. The dissociation of small biopsies will give volunteers a more comfortable experience as a subject of studies here at UW-Madison. Beyond patient comfort, if lung tissue can be successfully dissociated and allow for the analysis of

eosinophils, it may allow for the development or guidance of new treatments which will lead to better patient outcomes.

XI. References

[1] University Of Wisconsin - Department of Medicine. (2017). *Asthma: UW Research and You*. [online] Available at: https://www.medicine.wisc.edu/asthma/asthmamain [Accessed 10 Oct. 2017].

[2] Nigms.nih.gov. (2017). *Studying Cells - National Institute of General Medical Sciences*. [online] Available at: https://www.nigms.nih.gov/Education/Pages/FactSheet_Cells.aspx

[3] Office of the Associate Director for Communications (OADC), Centers for Disease Control (CDC), May 3, 2011, *Asthma in the US* [online]. Available at: https://www.cdc.gov/vitalsigns/asthma/index.html

[4] Hopkinsmedicine.org. (2017). *Lung Biopsy | Johns Hopkins Medicine Health Library*. [online] Available at: http://www.hopkinsmedicine.org/healthlibrary/test_procedures/pulmonary/lung_biopsy_92,P07750

[5] Miltenyibiotec.com. (2017). *gentleMACS™ Dissociator - Miltenyi Biotec*. [online] Available at: http://www.miltenyibiotec.com/en/products-and-services/macs-sample-preparation/tissue-dissociators-and-tubes/gentlemacs-dissociator.aspx

[6] Qiu, X., De Jesus, J., Pennell, M., Troiani, M. and Haun, J. (2017). Microfluidic device for mechanical dissociation of cancer cell aggregates into single cells. [online] PubMed.gov. Available at: https://www.ncbi.nlm.nih.gov/pubmed/25377468

[7] L. Jiang, R. Kraft, L. Restifo et al. " Dissociation of brain tissue into viable single neurons in a microfluidic device," [Online] Available: http://ieeexplore.ieee.org/document/7492500/. [Accessed: 21-Feb-2018].

[8] J. R. Murdoch and C. M. Lloyd, "Chronic inflammation and asthma," *Mutation Research*, 07-Aug-2010. [Online]. Available:

[9] S. Holgate, "Pathogenesis of Asthma", Clinical & Experimental Allergy, vol. 38, no. 6, pp. 872-897, 2008.

[10] S. Mathur, P. Fichtinger, M. Evans, E. Schwantes and N. Jarjour, "Variability of blood eosinophil count as an asthma biomarker", Annals of Allergy, Asthma & Immunology, vol. 117, no. 5, pp. 551-553, 2016.

[11] S. Holgate, S. Wenzel, D. Postma, S. Weiss, H. Renz and P. Sly, "Asthma", Nature Reviews Disease Primers, p. 15-25, 2015].

[12] "Bronchoscopy", Sanchest.com, 2018. [Online]. Available: http://www.sanchest.com/bronchoscopy.html. [Accessed: 01- May- 2018].

[13] "Multi-color flow cytometry | Expedeon | Application Notes", Expedeon, 2018. [Online]. Available: https://www.expedeon.com/application-notes/multi-color-flow-cytometry. [Accessed: 01- May- 2018].

[14] C. Yap, N. Saikrishnan and A. Yoganathan, "Experimental measurement of dynamic fluid shear stress on the ventricular surface of the aortic valve leaflet", Biomechanics and Modeling in Mechanobiology, vol. 11, no. 1-2, pp. 231-244, 2011.]

[15] "Lung Biopsy," *Lung Biopsy | Johns Hopkins Medicine Health Library*. [Online]. Available: http://www.hopkinsmedicine.org/healthlibrary/test_procedures/pulmonary/lung_biopsy_92,P07750.

[16] "What is Flow Cytometry?" [Online]. Available: https://www.news-medical.net/life-sciences/What-is-Flow-Cytometry.aspx. [Accessed: 06-Mar-2018].

[17] "Multi-color flow cytometry | Expedeon | Application Notes", Expedeon, 2018. [Online]. Available: https://www.expedeon.com/application-notes/multi-color-flow-cytometry. [Accessed: 01-May- 2018].

[18] J. D. C. Kimberly, et al. "Distribution of Lung Cell Numbers and Volumes between Alveolar and Nonalveolar Tissue," *Am. Rev. Respir. Dis.*, vol. 146, no. 2, pp. 454–456, 1992.

[19] E. R. W. James, et al. "Cell Number and Cell Characteristics of the Normal Human Lung," *Am. Rev. Respir. Dis.*, vol. 126, no. 2, pp. 332–337, 1981.

[20] C. Yap, N. Saikrishnan and A. Yoganathan, "Experimental measurement of dynamic fluid shear stress on the ventricular surface of the aortic valve leaflet", Biomechanics and Modeling in Mechanobiology, vol. 11, no. 1-2, pp. 231-244, 2011.

[21] H. Lu, L. Koo, W. Wang, D. Lauffenburger, L. Griffith and K. Jensen, "Microfluidic Shear Devices for Quantitative Analysis of Cell Adhesion", Analytical Chemistry, vol. 76, no. 18, pp. 5257-5264, 2004.

[23] C. M. B. Ho, et al. "3D printed microfluidics for biological applications," *Lab Chip*, vol. 15, no. 18, pp. 3627–3637, Aug. 2015.

[24] S. Waheed et al., "3D printed microfluidic devices: enablers and barriers," Lab Chip, vol. 16, no. 11, pp. 1993–2013, May 2016.

[25] F. Zhu, N. P. Macdonald, J. M. Cooper, and D. Wlodkowic, "Additive manufacturing of lab-on-a-chip devices: promises and challenges," 2013, vol. 8923, p. 892344.

[26] S. Takenaga *et al.*, "Fabrication of biocompatible lab-on-chip devices for biomedical applications by means of a 3D-printing process," *Phys. status solidi*, vol. 212, no. 6, pp. 1347–1352, Jun. 2015.

[27] J. Friend and L. Yeo, "Fabrication of microfluidic devices using polydimethylsiloxane", 2010. [Online]. Available: https://www.ncbi.nlm.nih.gov/pmc/articles/PMC2917889/. [Accessed: 07- Mar- 2018].

[28] A. G. Koutsiaris et al., “Volume flow and wall shear stress quantification in the human conjunctival capillaries and post-capillary venules in vivo.,” Biorheology, vol. 44, no. 5–6, pp. 375–86, 2007.

X. Appendix

Appendix A: Product Design Specifications

Microscale Tissue Biopsy Dissociation Device
Product Design Specifications
2018/3/7

Raven Brenneke, Nathan Richman, Lauren Ross, Thomas Guerin, Chrissy Kujawa

Function: To dissociate cells from small (1-2 mm^3) lung biopsy samples. The design must produce a measurable amount of viable cells for flow cytometry (approximately 10,000 white blood cells).

Client Requirements:

- Dissociate cells from lung biopsy samples retrieved from asthma patients during the duration of the asthma research study.
- Must be able to recover cells with minimal disruption to surface markers, so that the cells can be analyzed via flow cytometry.

Design Requirements:

1. Physical and Operational Characteristics

a. Performance Requirements: The device should successfully dissociate tissue samples to obtain at least 10,000 cells, ideally 10,000 white blood cells. The device will be used daily by lab technicians using sterile techniques to load tissue and unload cells.

b. Safety: The device must be sterile and protect the lab tech from possible contamination due to the use of human tissue samples. The device should also be able to withstand spills and drops without shattering or breaking into sharp shards.

c. Accuracy and Reliability: The device must yield at least 10,000 cells from the sample of tissue. It should completely dissociate the tissue samples without disrupting cell markers and not resulting in cell lysis.

d. *Life in Service*: Life in service will depend on whether or not the device is reusable. If it is reusable it needs to last enough runs so that the cost per use is less than $10. If non-reusable, it would only need to last for a single tissue dissociation.

e. *Shelf Life:* While not in use the device should have a shelf-life of at least 5 years in case the client's study ends and starts up later.

f. *Operating Environment*: The device will be used in a laboratory setting. During use, the device will be exposed to various enzyme-containing solutions including collagenase G, sterilization agents, and possibly high temperatures and pressures present in an autoclave (if device is reusable, it should withstand temperatures of -20 to 130 °C).

g. *Ergonomics*: The device must be simple for lab technicians to control. This includes being able to easily load a sample into the microfluidic device and unload the output from it.

h. *Size*: The device should be capable of dissociating a tissue sample size of 1-2 mm^3. The device should be able to fit on a lab bench, but otherwise, the size of the device is not of huge concern as long as it is able to perform the task successfully.

i. Weight: The weight of the device is currently not applicable to the design criteria given by the client's wishes. The microfluidic device is small enough that weight will not be a factor in its utility.

j. *Materials*: The material for the device must be cheap enough to obtain the goal of the cost per run being less than $10. The materials used will depend on the final fabrication method chosen. The material will need to not induce any inflammatory reaction with the cells. The current material used is PLA and ABS.

k. *Aesthetics*, *Appearance, and Finish*: The device must be simple and not confusing to use. The specific aesthetics and appearance of the final product is not of large concern as long as the device functions properly.

2. Production Characteristics

a. *Quantity*: The client initially requested one device to be manufactured for use, but an additional device may be requested later on.

b. *Target Product Cost*: The budget for this project is $300 dollars. The cost of fabrication of the device will be determined at later time depending on the type of material, volume of material, and fabrication technique selected. The existing device is non-reusable and costs roughly $10 per

cap with the tubes accompanying the device costing $6 per tube[1]. The target cost of the microfluidic device is $5-$10 per use.

3. Miscellaneous

a. *Standards and Specifications*: This is a custom device being used in a research setting; there are no international or national standards to abide by.

b. *Customer*: The client would prefer to have a removable lid on the device in order to remove potentially valuable tissue samples if the device does not run correctly.

c. *Patient-related concerns*: Patients will not be using this device; it will be used in a research setting. There is no storage of patient data incorporated in this device and the devices should be sterile with every use.

d. *Competition*: A current device for tissue dissociation is made by Miltenyi that includes a tube cap with an attached grinding component that is compatible with a machine, gentleMACS™, that initiates the grinding of the tissue. This device is currently used by the client, but since their tissue sample size is very small it is unable to be properly dissociated by the gentleMACS [3].

PDS References:

1. Miltenyibiotec.com. (2017). *gentleMACS™ M Tubes - Miltenyi Biotec*. [online] Available at: http://www.miltenyibiotec.com/en/products-and-services/macs-sample-preparation/tissue-dissociators-and-tubes/gentleMACS™-dissociators/gentleMACS™-m-tubes.aspx [Accessed 21 Sep. 2017].
2. Thermofisher.com. (2017). *Nunc™ 15mL & 50mL Conical Sterile Polypropylene Centrifuge Tubes*. [online] Available at: https://www.thermofisher.com/order/catalog/product/339650?SID=srch-srp-339650 [Accessed 21 Sep. 2017].
3. R.-P. D. Peters, E. D. Kabaha, W. Stöters, G. Winkelmayer, and F. G. Bucher, “Device for fragmenting tissue,” EP 2 540 394 B1, 2016.

Appendix B. Protocols

Fabrication of the Device:

1. Using Accura 60 material, the device was printed using a Viper SLA printer which took about 2 hours.
2. Once it finishes printing it cures in the printer itself for another hours.
3. The remaining resin is then drained and the part is taken out of the machine.
4. The supports are removed with a knife and the it is washed using denatured alcohol and an air pump to remove liquid from the channels. This is done about 10 times until clean.
5. The device is then put into a UV chamber for 2 hours.

Fabrication of the Silicone Gaskets:

1. Using the solidworks file, we re-created the single feature we needed for the gasket.
2. This file was converted to .dxf and loaded into the lasercutter software.
3. 1/16" silicone was washed with water, dried, then loaded into the cutter.
4. The system was set to the correct settings and 4 gaskets were cut.
5. Once they were finished (less than 2 minutes) they were removed and washed with soap and water.

Fabrication of the Input/Output Adaptors:

1. Device was clamped in place on a drill press in the TEAM Lab.
2. A 0.136” diameter (size 29) drill bit was inserted into the drill head.
3. Holes will drilled at each end of the device, in approximately the middle of the cross-section.
4. 0.136” diameter adaptors were inserted into the hole on each end of the device.
5. These adaptors were glued in place with superglue obtained from the TEAM Lab.

Assembly of Device for Testing:

1. 3D printed device was placed on the lab counter a few inches from the edge.
2. Sterilize the device with 70% ethanol by spraying all of the channels.
3. Rinse the device with water to remove the ethanol.
4. Input tubing was attached to the adaptor at one end of the device.
5. Output tubing was attached to the adaptor at the second end of the device.
6. Input tubing was laced into the peristaltic pump.
7. Tissue sample was placed in the device (the placement location varied with round of testing).
8. A silicone gasket was placed into the indentation of the channels.

9. A rubber sheet was placed above the silicone gasket.
10. The acrylic cover was placed above the rubber sheet.
11. The entire system was secured with the addition of three bar clamps (one at each end and one in the middle of the device).

Generic Microfluidic Device Testing Protocol (for 1 sample):

1. Obtain mouse lung tissue sample from Dr. Mathur's laboratory.
2. Allow the tissue to thaw if necessary (for frozen tissue).
3. Obtain sample biopsy (~12 mm^3) with a biopsy tool obtained from Dr. Mathur's laboratory.
4. Create collagenase solution in 10 mL conical tube for one sample. 20x Buffer S, Enzyme B, and Enzyme A are proprietary items obtained from the Miltenyi gentleMACS dissociator kit.
    a. 120uL 20x Buffer S
    b. 100uL Enzyme B
    c. 15uL Enzyme A
    d. 2.28mL 1x PBS
5. Place biopsy into the collagenase solution.
6. Place conical tube on a gentle rocking device and set in 37°C incubator for 45 minutes.
7. While incubating, begin assembling the device for testing (protocol above).
8. Add 2.5 mL 1x PBS to conical tube to make total volume ~5 mL.
9. Place proximal end of input tubing into conical tube solution.
10. Place distal end of output tubing into collecting tube, a 10 mL conical tube.
11. Turn on the peristaltic pump (either old pump or new pump) and run the entire 5 mL of solution through the device and into the collecting tube.
12. Switch the conical tubes connected to the input and output tubing.
13. Run the 5 mL of solution through the device again.
14. Retrieve the undissociated tissue from the device and add to the collecting tube.
15. Vortex the collecting tube for 5 seconds.
16. Filter the solution using a 50 micron filter (some testing was done without filtering)
17. Centrifuge the solution at 20°C and 1300 rpm for 10 minutes.
18. Remove as much supernatant as possible.
19. Resuspend the pellet in 1 mL of 1x PBS.
20. Dilute 20 µL of solution into 10 mL of cell counting solution.
21. Add 3 drops of red blood cell neutralizing solution.
22. Confirm that the coulter counter is set to measure particles between 4 and 7 µm.
23. Remove background signal by counting a blank sample on the coulter counter.
24. Count the diluted solution three times.
25. Record counting results.

Original Protocol for the Miltenyi GentleMACS Dissociator:

1. The tissue sample was about 1.5 inches in diameter (this sample was VERY large compared to what they usually get for this study)
2. Took 4 smaller biopsies with a biopsy tool
3. Two samples were placed in a 50 ml conical tube containing only 1x PBS solution
4. Two samples were placed in a 50 ml conical tube containing 1x PBS, 20x Buffer S, Enzyme A, Enzyme D
    a. 20x Buffer S, Enzyme A, Enzyme D are all from the dissociation kit that came with the GentleMACS device
5. Samples were then placed in the incubator for 30 minutes on a gentle rocking device
6. Conical tubes were vortexed for 5 seconds
7. Solution was filtered using a 50 micron filter
8. Tubes were centrifuged at room temp, 1300 rpm for 10 minutes
9. Supernatant was taken off, and cell solution at the bottom of the tube was resuspended in PBS and loaded into cytospin device
10. Centripetal force from that device forced cells onto glass slide
11. Slide was stained with HEMA 3

Determination of Biopsy Volume with ImageJ:

1. An image of the samples for final testing was taken using a ruler as a scale bar.
2. The average thickness of each of the samples was ~1 mm.
3. A line of known length (10 mm) was drawn in ImageJ using the ruler image as reference.
4. ImageJ assigned the number of pixels in that line to the reference length.
5. Each tissue sample was then outlined.
6. The measure function within ImageJ was used to determine the surface area of each outlined tissue sample.
7. Three surface area measurements were taken for each sample and averaged.
8. By multiplying the calculated average surface area by the approximate thickness (1 mm), the approximate volume of each sample was determined.

Appendix C: Programmable Peristaltic Pump

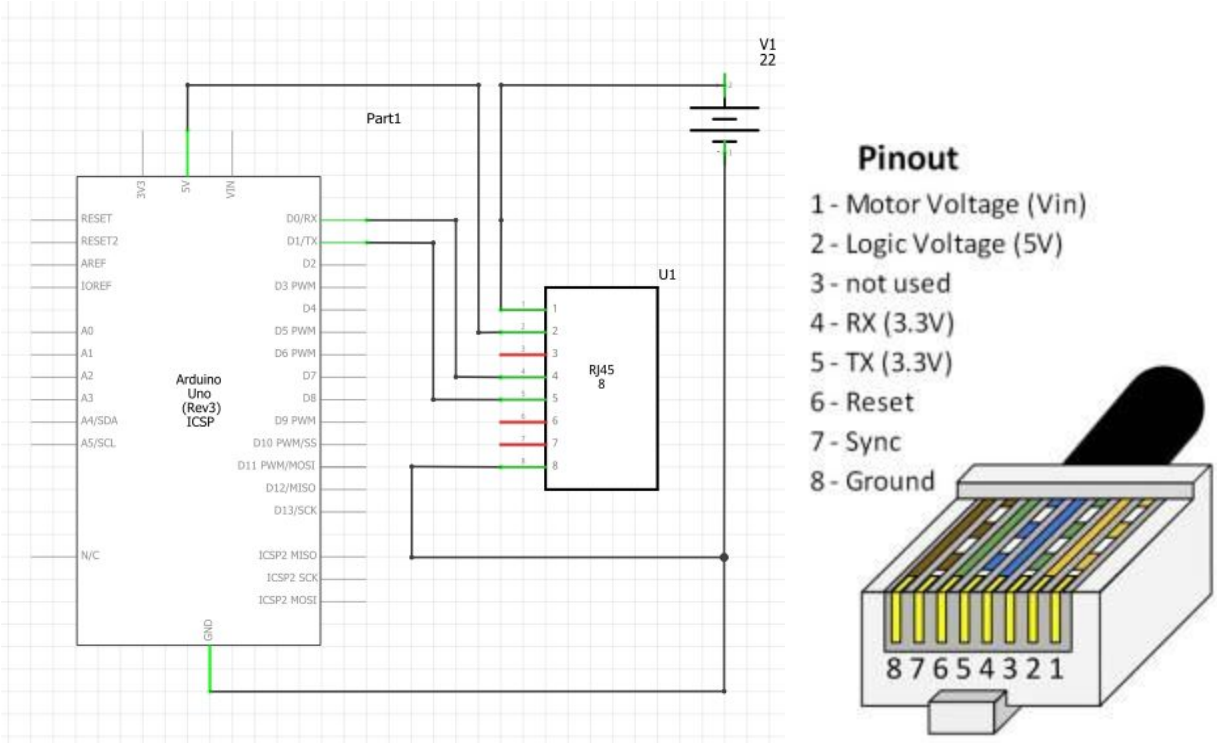

Figure 1: Circuit diagram for Arduino connected to pump. Arduino is connected to the RJ-45 adaptor, the RX and TX pins are connected to their respective pin on the Arduino, the logic voltage is connected, as well as the external motor voltage (22V), all is then grounded to that voltage source.

Initial arduino code to control pump:

```
#include <SoftwareSerial.h>
SoftwareSerial mySerial(0,1); //RX, TX

void setup() {
  pinMode(0,INPUT); //Set input and output modes
  pinMode(1,OUTPUT);
  mySerial.begin(9600);
  delay(100); //Delay after setting up serial
}

void loop() {

mySerial.println("!!!");          //Send start signal to pump (from datasheet)
delay(1000);                      //Todo: find a way to only send start signal once
mySerial.write("speed 100 1\n\r");    //Send signal to start, delay, then tell pump forward
delay(50);                              //Might need to switch order around, i.e. forward first
```

```
mySerial.write("forward\n\r");          //then speed
  delay(50);
  mySerial.write("timedisp 1000\n\r");          //Tell it to run for 4 seconds, then tell it to run
  delay(4000);                                  //backward for 4 seconds
  mySerial.write("backward\n\r");
  delay(50);
  mySerial.write("timedisp 1000\n\r");
  delay(4000);
}
```

Appendix D: Project Materials/Finances

Item	Description	Manufacturer	Part Number	Date	QTY	Cost Each	Total
Bar Clamp	Obtained from TEAM Lab	N/A	N/A	3/12/18	3	$0.00	$0.00
Final Tissue Dissociation Device	3D Print material: Accura 60	Morgridge Fab Lab	N/A	3/16/18	1	$35.00	$35.00
Silicone Gasket	Lasercut from silicone	Morgridge Fab Lab	N/A	3/16/18	4	$0.00	$0.00
Acrylic Cover	Obtained from TEAM Lab	N/A	N/A	3/20/18	1	$0.00	$0.00
Handcut Rubber Gasket	Obtained from TEAM Lab	N/A	N/A	4/6/18	1	$0.00	$0.00
Final Poster Printing		Steenbock Library	N/A	4/26/18	1	$48.00	$48.00
						TOTAL:	**$83.00**

Appendix E: Flow calculations

Micro/macroscopic flow analysis for microfluidic tissue dissociation device

Raven Brenneke, Tommy Guerin, Chrissy Kujawa,
Nathan Richman, Lauren Ross

April 21, 2018

1 Microscopic analysis

1.1 Narrow Region

Using the navier-stokes equations, we can simplify the x and y components of the momentum balances in Figure 1 with the assumptions that we are at steady state (1), the velocity is a function of x and y only (2) and that the liquid has a constant viscosity and density (3), i.e. isothermal system:

$$\rho\left(v_x\frac{\partial v_x}{\partial x}+v_y\frac{\partial v_x}{\partial y}\right)=-\frac{\partial p}{\partial x}+\mu\left[\frac{\partial^2 v_x}{\partial x^2}+\frac{\partial^2 v_x}{\partial y^2}\right]$$
$$\rho\left(v_x\frac{\partial v_y}{\partial x}+v_y\frac{\partial v_y}{\partial y}\right)=-\frac{\partial p}{\partial y}+\mu\left[\frac{\partial^2 v_y}{\partial x^2}+\frac{\partial^2 v_y}{\partial y^2}\right]$$

These PDE's are very difficult to solve simultaneously, even with the relations given above by the continuity equation, therefore for particular velocities and stresses, we will need to use finite element analysis.

Simplification Because the above PDE's are too difficult to solve for velocity profiles, we can make more simplifications and look at an area where the flow is approximately pressure driven flow between two plates. Therefore we can assume that the velocity is in the x direction, and that it is a function of y. Pressure however, is still a function of x, but we only need to solve the x-component of the momentum balance, which simplifies to:

$$\frac{dp}{dx}=\mu\left(\frac{d^2 v_y}{dy^2}\right) \tag{1}$$

1

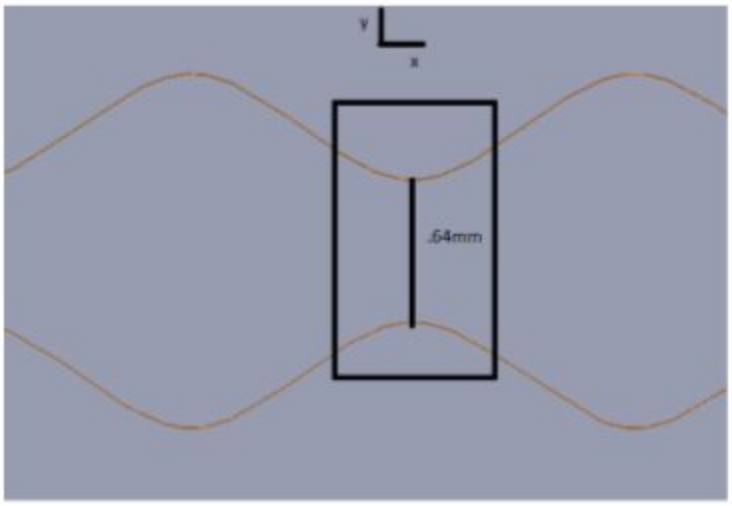

Figure 1: Illustration of narrow section of channel. The curved narrow region can be approximated as a small region of pressure driven flow between two flat plates.

Since we have a two differential equations with respect to 2 different variables, x and y, they must be equal to a constant of separation, B.

$$\frac{dp}{dx} = \mu\frac{d^2v_x}{dy^2} = B$$
$$\frac{dp}{dx} = B$$
$$\mu\frac{d^2v_x}{dy^2} = B$$

We can then separate the equations and solve the pressure equation to find B:

$$\int_{p_0}^{p_1} dp = B\int_{x_0}^{x_1} dx$$
$$\frac{(p_1 - p_0)}{L} = B$$

We can then substitute B back into the equation for v_x

$$\frac{d^2v_x}{dy^2} = \frac{(p_1 - p_0)}{\mu L}$$
$$v_x(y) = \frac{(p_1 - p_0)}{\mu L}y^2 + c_1y + c_2$$

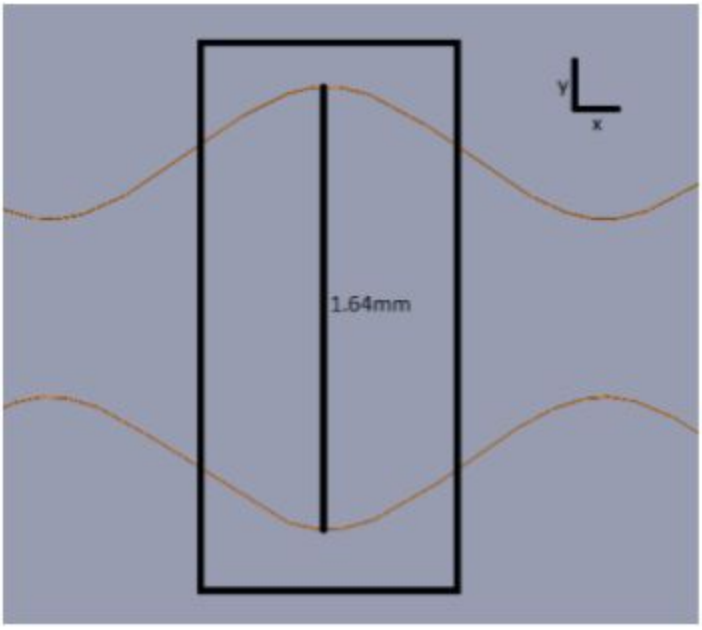

Figure 2: Illustration of narrow section of channel. The curved narrow region can be approximated as a small region of pressure driven flow between two flat plates.

Applying the boundary conditions $v_x(-h) = 0$ and $v_x(h) = 0$, where thickness is 2h we can solve for the velocity profile. We can then apply Newtons law of viscosity $\tau_{yx} = -\mu\frac{\partial v_x}{\partial y}$ to solve for the shear stress distribution:

$$v_x(y) = \frac{(p_0 - p_1)h^2}{2\mu L}\left(1 - \left(\frac{y}{h}\right)^2\right) \tag{2}$$

$$\tau_{yx} = \frac{(p_0 - p_1)}{L}y \tag{3}$$

1.2 Wide Region

The same problem fan be formulated for the wide region of the channel, Figure 2 The only difference in solution would be the value of h in the above equation.

1.3 Comparison

In order to compare the wide and small sections we need to find their volumetric flow rate. The flow rate can be found by integrating the velocity

profile along a characteristic cross-sectional area.

$$Q = \iint v_x(y)dA = 2 * \int_0^D \int_0^h \frac{(p_0 - p_1)h^2}{2\mu L}\left(1 - \left(\frac{y}{h}\right)^2\right)dydz \tag{4}$$

$$Q = \frac{2D\Delta ph^2}{2\mu L}\left[y - \frac{y^3}{3h^2}\right]_0^h \tag{5}$$

$$= \frac{2D\Delta ph^2}{2\mu L}\left[h - \frac{h^3}{3h^2}\right] \tag{6}$$

$$= \frac{2D(\Delta p)h^3}{3\mu L} \tag{7}$$

With a Q of 1mL/s we can then analyze the pressure needed to create these flows, as well as the maximum velocities and shear stresses:

Wide section:

$$1 * 10^{-6}m^3/s = \frac{2 * .010m * (\Delta p) * (.00082m)^3}{3 * 1 * 10^{-3}Pa * s * .001m}, \Delta p = .272Pa \tag{8}$$

$$v_{max} = \frac{(\Delta p)h^2}{2 * \mu L} = \frac{.272Pa * (.00082m)^2}{2 * 1 * 10^{-3}Pa * s * .001m} = .182m/s \tag{9}$$

$$t_{xz}^{max} = \frac{\Delta p * y}{L} = \frac{.272Pa * .00082m}{.001m} = .223N/m^2 \tag{10}$$

Thin section:

$$1 * 10^{-6}m^3/s = \frac{2 * .010m * (\Delta p) * (.00032m)^3}{3 * 1 * 10^{-3}Pa * s * .001m}, \Delta p = 4.577Pa \tag{11}$$

$$v_{max} = \frac{(\Delta p)h^2}{2 * \mu L} = \frac{4.577Pa * (.00032m)^2}{2 * 1 * 10^{-3}Pa * s * .001m} = .234m/s \tag{12}$$

$$t_{xz}^{max} = \frac{\Delta p * y}{L} = \frac{4.577Pa * .00032m}{.001m} = 1.46N/m^2 \tag{13}$$

The thin section requires a much larger pressure difference to create the same volumetric flow rate, which is expected. This causes the v_{max} to be larger as well as the maximum shear stress.

2 Macroscopic balance

We can approximate flow rate and velocities at entrance and exit by using macroscopic balances. The macroscopic mass, momentum and mechanical energy balances are shown below for an isothermal system:

$$\sum\left(\rho_1 \langle v_1 \rangle S_1\right) - \sum\left(\rho_2 \langle v_2 \rangle S_2\right) = 0 \tag{14}$$

$$F_{f\to s} = -\Delta\left(\frac{\langle v^2 \rangle}{\langle v \rangle} + pS\right)\underline{y} + m_{tot}g \tag{15}$$

Figure 3: Macroscopic balance set up. We pick two planes that have the same cross sectional area S. We can then do macroscopic balances on this section of the channel to find forces of the fluid on the solid to approximate shear forces and flow rates.

$$\Delta\left(\frac{1}{2}\frac{\langle v^3\rangle}{\langle v\rangle}\right) + g\Delta h + \int_1^2 \frac{dp}{\rho} = \hat{W}_m - \hat{E}_v \tag{16}$$

Since there are no moving surfaces in this system, $\hat{W}_m$ can be neglected. Secondly since our solution will be water based, we can assume incompressible flow, so that ρ is not a function of pressure, then the integral term becomes $\frac{p_2-p_1}{\rho}$, and finally, since our design does not change in height, we can exclude the gravitational potential energy term in the mechanical energy balance. We assume that the flow is isothermal and that the density does not change. Since we picked planes with equal cross sections, we can see from the mass balance that $\langle v_1\rangle = \langle v_2\rangle = \langle v\rangle$ Then we can further simplify the mechanical energy balance to the following:

$$\frac{\Delta p}{\rho} + \hat{E}_v = 0 \tag{17}$$

We can assume that the shapes in the channel can be approximated by using friction factor terms for sudden contractions and sudden expansions:

$$\hat{E}_v = \sum^{i} 1/2v^2 * (.45(1-\beta)) + \sum^{j} 1/2v^2 * (\frac{1}{\beta} - 1)^2 \tag{18}$$

where β is the ratio of the small to large cross sectional area: $6.4mm^2/16.4mm^2 = .3902$. We can get $\langle v\rangle$ from the analysis above. For the sudden expansions, $\langle v\rangle$ is just the spacially averaged velocity from the thin section, whereas for

the sudden contractions it is the spacially averaged velocity from the wide section. Where $\langle v \rangle$ is given by $2/3 v_{max}$

$$\begin{aligned}\hat{E_v} &= i\left(\frac{1}{2}(\frac{2}{3} * .182\frac{m}{s})^2(.45(1-.3902))\right) + j\left(\frac{1}{2}(\frac{2}{3} * .234\frac{m}{s})^2(\frac{1}{.3902}-1)^2\right) \\ &= i * .00202m^2/s^2 + j * .0297m^2/s^2\end{aligned}$$

In the smallest channel of our design, we have 18 sudden contractions and 18 sudden expansions, we can now use this to calculate the pressure drop along one of these channels.

$$\frac{\Delta p}{1000kg/m^2} = 18 * .00202m^2/s^2 + 18 * .0297m^2/s^2 \tag{19}$$

$$\Delta p \approx 570.96Pa = .083lb_f/in^2 \tag{20}$$

Thus with a flow rate of 1ml/s, the smaller channels would have a pressure drop of about .083 psi

Appendix F: Raw Data From Testing

Comparison of filtered vs non-filtered

Filtered - cell counts

Sample 1	28000	32500	44000
Sample 2	49500	40500	46000
Sample 3	87000	94000	68000
Sample 4	134500	120500	117000
Sample 5	65000	65000	62500
Sample 6	52400	48400	52400
Sample 7	124800	117600	42800

Non-filtered - cell counts

Sample 1	249500	336500	217000
Sample 2	128000	125000	125500
Sample 3	99000	60000	
Sample 4	131000	167000	
Sample 5	106500	92000	84000

Comparison of old pump vs new pump

Old pump - cell counts

Sample 1	99000	60000	
Sample 2	131000	167000	
Sample 3	106500	92000	84000

New pump -cell counts

Sample 1	52400	48400	52400
Sample 2	124800	117600	42800
Sample 3	28000	32500	44000

Sample 4	49500	40500	46000
Sample 5	87000	94000	68000
Sample 6	134500	120500	117000
Sample 7	65000	65000	62500

Comparison of fresh tissue vs frozen tissue

Fresh tissue - cell counts

Sample 1	3.65E+05	5.07E+05	4.74E+05
Sample 2	201000	272700	254400

Frozen tissue - cell counts

Sample 1	99000	60000	
Sample 2	131000	167000	
Sample 3	106500	92000	84000

Comparison of Different Testing Conditions

ImageJ analysis (surface area in mm^2)

	Measure 1	Measure 2	Measure 3	Average
A	25.69	19.448	22.396	22.51133333
B	13.58	15.006	22.036	16.874
C	24.182	20.941	18.367	21.16333333
D	16.567	15.726	12.605	14.966
E	7.495	8.403	10.204	8.700666667
F	13.633	10.549	14.953	13.045
G	7.923	6.723	6.55	7.065333333
H	6.91	8.058	9.911	8.293

I	8.351	8.951	8.816	8.706
J	14.233	12.793	9.431	12.15233333
K	9.776	13.19	17.287	13.41766667
L	16.206	14.286	13.459	14.65033333

*Numbers converted to mm^3 by multiplying by 1mm thickness of the samples

Cell counts measured for each label

Tissue #	Cell Count #1 (4-7)	Cell Count #2 (4-7)	Cell Count #3 (4-7)
A Device 1	56000	65000	88000
B Device 2	99000	81000	92000
C Device 3	174000	188000	136000
D Device 4	269000	241000	234000
E Device 5	130000	130000	125000
F Device 1 with pellet	499000	673000	434000
G Device 2 with pellet	256000	250000	251000
H Miltenyi 1	165000	195000	165000
I Miltenyi 2	299000	256000	227000
J Miltenyi 3	401000	378000	400000
K Miltenyi 4	529000	426000	399000
L Miltenyi 5	1078000	1046000	966000